2023 IEEE/ASME International Conference on Advanced Intelligent Mechatronics (AIM)
June 28-30, 2023. Seattle, Washington, USA

Ensemble Control for Manipulating Multiple Nanowires in Fluid Suspension Using External Electrical Fields

Juan Wu and Kaiyan Yu

***Abstract*— This paper presents an ensemble control system for precise online manipulation of micro- and nanoscale objects. Existing wireless external actuation approaches exhibit global and coupled influences, hindering robust and simultaneous control of multiple particles. The proposed system incorporates the rotational dynamics of nanowires in fluid suspension and offers two control methods: a two-stage open-loop ensemble control law and a model-predictive ensemble control strategy. Simulation results demonstrate that both methods surpass the theoretical limits of simultaneous particle control. The model-predictive ensemble control method can control more nanowires, does not require pre-generated trajectories, and has a simpler validation process for control performance.**

I. Introduction

Efficient manipulation of microscopic objects is essential for numerous research applications. However, traditional tools such as tip-based or optical tweezers lack the ability to simultaneously steer multiple objects effectively. Field-based actuation, such as magnetic or electric fields, has shown promise in remote control for various applications, including medical procedures and micro-, nano-, and bio-manipulations. Despite the introduction of several micro- and nanomanipulation techniques, field-based manipulation methods suffer from the global and coupled influences of the wireless external actuation in the workspace, limiting the capability to robustly control multiple micro- and nanoparticles independently and simultaneously [1]. Various approaches have been proposed to achieve automated transport of micro- and nanoagents under a global input, including electrostatic anchoring [2], local field decoupling [3], non-uniformity of the robots [4], and heterogeneity of the agents [5]. However, there has been no systematic investigation of the maximum number of agents that can be simultaneously and independently controlled with global field inputs.

Ensemble control theory aims to control a group of dynamic systems with different parameters using the same control signal [6]. This approach has applications in quantum systems and involves maintaining a set of all possible configurations of the system and choosing the same input at each step to steer the entire system to a neighborhood of the target configuration [7]. The controllability of an ensemble system can be studied by looking at the algebra of polynomials defined by the noncommuting vector fields that govern the system dynamics [8]. The Lie algebra rank condition can be used to prove nonlinear ensemble controllability.

This work was supported by the NSF under Award CMMI 2146056.

J. Wu and K. Yu are with the Department of Mechanical Engineering, Binghamton University, Binghamton, NY 13902 USA (email: jwu123@binghamton.edu; kyu@binghamton.edu).

At low Reynolds numbers, the translation motion of nanowires can be modeled in the form of $\dot{q}(t,\epsilon) = \epsilon \sum_{i=1}^{n} g_i(q(t,\epsilon))u_i(t)$, where q is the system states, ϵ is the varying parameter in the system dynamics, and is unique for each elements, n is the number of the elements, g_i represents the vector fields from the system dynamics, and u_i is the input to the system. In [8], it is noted that the system is not ensemble-controllable if the Lie algebra generated by g_i is nipotent. This is due to the inability to generate a desired higher order power of ϵ from the Lie algebra using the translation motion model of the nanowires. However, in [7], a fictitious collection of unicycles with similar system dynamics was steered as an ensemble under a bounding unknown model perturbation. A reduced subsystem was derived by utilizing repeated bracketing and polynomial approximation to build arbitrary vector flows, making it ensemble-controllable.

This paper proposes an ensemble control scheme using a shared, global electric field to control multiple one-dimensional nanowires simultaneously and independently, inspired by [7]. The research aims to enable scalable nanomanufacturing of functional micro- and nanodevices [9]. The main contributions of the work are: (1) The paper validates the rotational model for a nanowire experiencing an external electric field in fluid suspension through experimental results and develops a new ensemble control problem by introducing the rotation motion of the nanowires. (2) Two control methods, two-stage open-loop ensemble control and model predictive ensemble control, are presented for controlling multiple nanowires to their independent targets. (3) The proposed control schemes break the limit on the maximum achievable number of nanowires that can be controlled with global field inputs, and their performance is verified through extensive simulation results. The proposed research methodologies are not limited to electric field actuation and can be generalized to other field-based applications where the actuation among a group of agents is coupled or intertwined.

II. Motion Model of Nanowires in Fluid Suspension under Electric Fields

A. Translational Model Formulation

As shown in Fig. 1(a), we consider n nanowires immersed in a viscous fluid under an external DC electric field. Denote the position of the ith nanowire as $\boldsymbol{r}_i(t) = [x_i(t)\ y_i(t)]^\intercal$, $i = 1, \cdots, n$ and the position vectors of all nanowires as $\boldsymbol{q}(t) = [\boldsymbol{r}_1^\intercal(t) \cdots \boldsymbol{r}_n^\intercal(t)]^\intercal \in \mathbb{R}^{2n}$. The equation of motion is given as follows [10]–[13]:

$$\dot{\boldsymbol{q}}(t) = \boldsymbol{Z}\boldsymbol{B}(\boldsymbol{q}(t))\boldsymbol{u}(t), \tag{1}$$

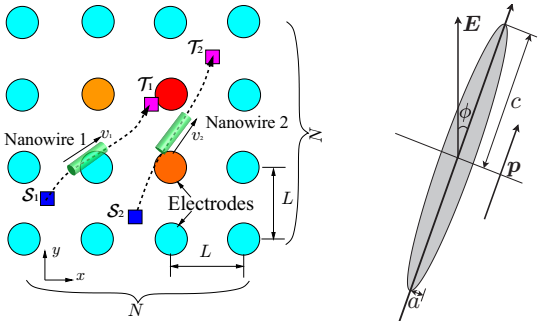

(a) (b)

Fig. 1. (a) Top-view of the schematic of the microfluidic device with $N \times N$ independently actuated electrodes on the bottom substrate. The array of circular electrodes with diameter $L/2$ is fabricated with equal distances L between the electrode centers as measured along the x and y axes. Each electrode is independently actuated with a DC voltage. (b) A nanowire is suspended in a fluid that is subjected to an external electric field $\boldsymbol{E}$.

where $\boldsymbol{Z} = \text{diag}[\zeta_{1x}, \zeta_{1y} \cdots \zeta_{nx}, \zeta_{ny}] \in \mathbb{R}^{2n\times 2n}$, $\begin{bmatrix}\zeta_{ix} & \zeta_{iy}\end{bmatrix}$ is the zeta potential of the ith suspended nanowire in x- and y-axis directions, respectively. $\boldsymbol{B} \in \mathbb{R}^{2n\times N^2}$ is the motion gain matrix:

$$\boldsymbol{B} = C \begin{bmatrix} \boldsymbol{E}_1(\boldsymbol{r}_1(t)) & \cdots & \boldsymbol{E}_{N^2}(\boldsymbol{r}_1(t)) \\ \vdots & \ddots & \vdots \\ \boldsymbol{E}_1(\boldsymbol{r}_n(t)) & \cdots & \boldsymbol{E}_{N^2}(\boldsymbol{r}_n(t)) \end{bmatrix}, \tag{2}$$

where $\boldsymbol{E}_j(\boldsymbol{r}_i(t)) = [E_{x_j}(\boldsymbol{r}_i(t))\ E_{y_j}(\boldsymbol{r}_i(t))]^\intercal$, $i = 1, \cdots, n$, $j = 1, \cdots, N^2$, is the DC electric field vector under unit voltage at $\boldsymbol{r}_i(t)$ by the jth electrode. $C = \varepsilon/\mu$, μ is the dynamic viscosity of the fluid, and ε is its electric permittivity. $\boldsymbol{u} = \{u_j\} \in \mathbb{R}^{N^2}$ is the corresponding controlled voltage that is applied to the $N \times N$ electrode array. Every two rows in Eq. (1) represent one nanowire's translational motion.

Given the desired target $\mathcal{T}$, we want to obtain $\boldsymbol{u}$ that subjected to $\|\boldsymbol{u}\|_\infty < u_{\text{bound}}$ to steer multiple particles to reach their targets, where u_{bound} is maximum bound of the applied voltages. From the above discussion, this control problem is not ensemble-controllable.

We added quadruple electrodes outside the bottom electrode array as shown in Fig. 2, where four phase-shifted AC voltages are applied with a sequential phase shift of 90° [14]. The rotational model of the nanowires in fluid suspension under external electric fields is formulated, where the nanowire rotation is achieved by applying AC fields to the quadruple electrodes. The frequency and magnitude of the AC field and nanowire's properties affect the rotational speed.

B. Rotational Model Formulation

The rotational rate of suspended nanowires under an external electric field is formulated as follows. Consider a conducting polarizable spheroid in an electrolyte that is subjected to a vertical electric field $\boldsymbol{E}$, as shown in Fig. 1(b). When the electric field $\boldsymbol{E}$ is applied, the nanowire rotates to align with the electric field's direction. Define a coordinate system such that the major axis of the spheroid, whose direction is given by a unit vector $\boldsymbol{p}$, lies in the plane, and without loss of generality, it can be assumed that both vectors $\boldsymbol{E}$ and $\boldsymbol{p}$ lie in the same plane. The angle formed by the electric field and the wire's major axis is ϕ, so $\boldsymbol{E}\cdot\boldsymbol{p} = E cos\phi$. Let $2c$ and $2a$ be the lengths of the major and minor axes of the spheroid, respectively. Denote the particle aspect ratio by $\gamma = c/a$ and its inverse by α. The rotation rate of the wire is influenced by two factors: slip velocity on particle surfaces and electro-rotational torque from the dipole moment [15]. From the slender-body theory in [15], the angular velocity induced by the normal component of the slip velocity on the particle surface can be expressed as $\boldsymbol{\Omega}_s = \frac{\varepsilon}{\mu}\boldsymbol{p} \times \tilde{\boldsymbol{E}}(\boldsymbol{p}\cdot\boldsymbol{E})$, where $\tilde{\boldsymbol{E}}$ is the circumferentially averaged and linearized electric field along the particle, and the detailed derivation can be found in [15]. In addition to the slip velocity induced angular velocity, $\boldsymbol{\Omega}_s$, rotation also occurs due to the interaction between the electric field and the dipole moment of the nanowire, which produces a torque through electro-rotation, and the resulting angular velocity is $\boldsymbol{\Omega}_e = \frac{\varepsilon log 2\gamma}{\mu\gamma^2}\tilde{\boldsymbol{E}} \times \boldsymbol{E}$. As a result, the angular velocity of the nanowire $\boldsymbol{\Omega} = \boldsymbol{\Omega}_s + \boldsymbol{\Omega}_e$.

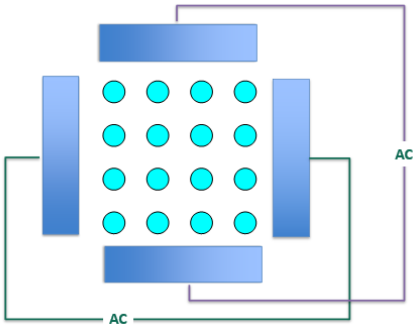

Fig. 2. Top-view of the schematic of the microfluidic device with $N \times N$ DC electrodes and quadruple AC electrodes.

C. Model Validation by Experiments

The translation model has been validated in our previous work [16]–[19]. Experimental validation of the rotational model was performed by comparing the angles of nanowires captured by a high-resolution microscope camera to the numerically integrated angles from the derived model. Figs. 3(a) and 3(b) show the results of experiments with nanowires suspended in light and high viscosity mineral oil, respectively, with the electric field direction changing at a variable rate. The plots demonstrate that the nanowire continuously rotates to align with the field direction, and the angle results from the rotation model are consistent with the experimental data.

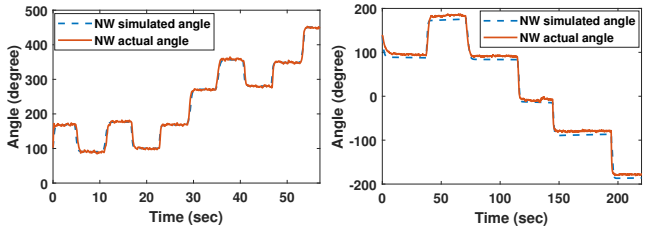

(a) (b)

Fig. 3. Experimental plots for silicon nanowires' orientations under a switching external electric field. (a) The nanowire rotates in light viscosity mineral oil. (b) The nanowire rotates in heavy viscosity mineral oil.

III. Ensemble Control Schemes

In this section, the microfluidic setup is rebuilt to create an ensemble-controllable system. As shown in Fig. 2, an $N \times N$ electrode array is fabricated on the substrate, and a set of quadruple electrodes is added outside the bottom electrode array. DC voltages are applied to each circular electrode independently to manipulate the nanowires' horizontal motion, while four phase-shifted AC voltages are simultaneously applied to the peripheral electrodes, which contribute to the rotation of the nanowires. The new system dynamics for the ith nanowire are given by

$$\begin{bmatrix}\dot{x}_i\\ \dot{y}_i\\ \dot{\theta}_i\end{bmatrix} = \begin{bmatrix}\zeta_{ix}\boldsymbol{B}_{2i\text{-}1}\\ \zeta_{iy}\boldsymbol{B}_{2i}\\ 0\end{bmatrix}\boldsymbol{u} + \begin{bmatrix}0\\0\\1\end{bmatrix}\Omega_i, \tag{3}$$

where x_i, y_i, θ_i, and Ω_i are the x-, y- positions, orientation, and angular velocity of the ith nanowire, respectively, without considering the disturbance. According to [14], applying an AC field with a fixed amplitude and frequency to the designed set of electrodes yields a constant angular velocity that varies for each individual nanowire. In the following section, we will demonstrate that this dynamic system is ensemble-controllable.

A. Ensemble Controllability by Polynomial Approximation

This section proves the ensemble-controllability of the revised microfluidic setup with certain constraints, similar to the proof for the subsystem in [7]. The system dynamics are shown in Eq. (3), where $\boldsymbol{u}$ is the voltage input vector to the electrodes, and $\boldsymbol{Bu}$ is the electric field vector at the nanowires' positions. The electric field can be expressed as $E_0[\cos(\theta_E)\ \sin(\theta_E)]^\intercal$, where E_0 is the magnitude of the electric field and θ_E is the angle of the electric field. The input field constraint is that the electric field direction must align with the rotating angle of the nanowires, i.e., $\theta_E = \theta_i$, to create an ensemble-controllable system. Therefore, the equation of motion for the individual nanowire can be expressed as

$$\begin{bmatrix}\dot{x}_i\\ \dot{y}_i\\ \dot{\theta}_i\end{bmatrix} = \begin{bmatrix}\cos(\theta_i)\\ \sin(\theta_i)\\ 0\end{bmatrix}\zeta_{ip}E_0 + \begin{bmatrix}0\\0\\1\end{bmatrix}\Omega_i, \tag{4}$$

where ζ_{ip} is the zeta potential for the nanowire along its longitudinal body direction, which is a unique constant for each nanowire.

Because the rotational rate of each nanowire is constant but varies due to its different geometric shapes, we can introduce an auxiliary state γ_i for the proof, where $\theta_i(t) = \theta_i(0)+\epsilon\gamma_i(t)$, and $\dot{\theta}_i(t) = \epsilon\dot{\gamma}_i(t)$. ϵ is the distribution parameter for each nanowire. Then the evolution of the system is governed by

$$\begin{bmatrix}\dot{x}_i\\ \dot{y}_i\\ \dot{\gamma}_i\end{bmatrix} = \begin{bmatrix}\cos(\theta_i(0)+\epsilon\gamma_i)\\ \sin(\theta_i(0)+\epsilon\gamma_i)\\ 0\end{bmatrix}\zeta_{ip}E_0 + \begin{bmatrix}0\\0\\1\end{bmatrix}\dot{\gamma}_i. \tag{5}$$

Denote the configuration of the system as $\boldsymbol{p}_i = [x_i\ y_i\ \gamma_i]^\intercal$, $h_1 = [\cos(\theta_i(0)+\epsilon\gamma_i)\ \sin(\theta_i(0)+\epsilon\gamma_i)\ 0]^\intercal$ and $h_2 = [0\ 0\ 1]^\intercal$, the system can be expressed as $\dot{\boldsymbol{p}}_i = \zeta_{ip}h_1u_1+h_2u_2$ with $u_1 = E_0$ and $u_2 = \dot{\gamma}_i$. Now we prove the ensemble controllability by using repeated bracketing to get higher order powers of ϵ and by using polynomial approximation to construct arbitrary vector flows. Taking Lie brackets, we have:

$$\begin{aligned}
[\zeta_{ip}h_1, h_2] &= \zeta_{ip}(\frac{\partial h_2}{\partial \boldsymbol{p}}h_1 - \frac{\partial h_1}{\partial \boldsymbol{p}}h_2)\\
&= 0 - \zeta_{ip}\begin{bmatrix}0 & 0 & -\epsilon\sin(\theta_i(0)+\epsilon\gamma_i)\\ 0 & 0 & \epsilon\cos(\theta_i(0)+\epsilon\gamma_i)\\ 0 & 0 & 0\end{bmatrix}\begin{bmatrix}0\\0\\1\end{bmatrix}\\
&= \zeta_{ip}\epsilon\begin{bmatrix}\sin(\theta_i(0)+\epsilon\gamma_i)\\ -\cos(\theta_i(0)+\epsilon\gamma_i)\\ 0\end{bmatrix}
\end{aligned}$$

Denote $h_3 = [-\sin(\theta_i(0)+\epsilon\gamma_i), \cos(\theta_i(0)+\epsilon\gamma_i)]^\intercal$, we can get $[\zeta_{ip}h_1, h_2] = -\zeta_{ip}\epsilon h_3$. As a result,

$$\begin{aligned}
[[\zeta_{ip}h_1, h_2], h_2] &= -\zeta_{ip}\epsilon(\frac{\partial h_2}{\partial \boldsymbol{p}}h_3 - \frac{\partial h_3}{\partial \boldsymbol{p}}h_2)\\
&= 0 + \zeta_{ip}\epsilon\begin{bmatrix}0 & 0 & -\epsilon\cos(\theta_i(0)+\epsilon\gamma_i)\\ 0 & 0 & -\epsilon\sin(\theta_i(0)+\epsilon\gamma_i)\\ 0 & 0 & 0\end{bmatrix}\begin{bmatrix}0\\0\\1\end{bmatrix}\\
&= -\zeta_{ip}\epsilon^2\begin{bmatrix}\cos(\theta_i(0)+\epsilon\gamma_i)\\ \sin(\theta_i(0)+\epsilon\gamma_i)\\ 0\end{bmatrix} = -\zeta_{ip}\epsilon^2 h_1.
\end{aligned}$$

We can raise the dispersion parameters $\cos(\gamma_i)$ and $\sin(\gamma_i)$ to higher powers, thereby achieving robustness with dispersion to ϵ by generating appropriate Lie brackets. This proves that the new system is ensemble-controllable under the constraint.

B. Two-stage Open-Loop Ensemble Control

In this section, a two-stage open-loop ensemble control law is derived by separating the control process into two stages under the assumption that the zeta potentials of each nanowire are known parameters. In the first stage, a k-step control law is developed to determine the desired sequence of k control inputs for the magnitude of the electric fields to reach the goal state. In the second stage, the voltage input is solved to obtain the desired electric field strength at the nanowires' configurations, assuming that the electric field aligns with the nanowire's orientation during its motion.

1) First Stage: We express the system dynamics as a discrete-time model in Eq. (6) with k as the time step, x and y as the nanowire positions in the x- and y-directions, $\theta_i(k)$ as the nanowire's orientation angle at the kth step, and dt as the time interval per step:

$$\begin{bmatrix}x_i(k+1)\\ y_i(k+1)\end{bmatrix} = \begin{bmatrix}x_i(k)\\ y_i(k)\end{bmatrix} + \zeta_{ip}\begin{bmatrix}\cos(\theta_i(k))\\ \sin(\theta_i(k))\end{bmatrix}E_0(k)dt. \tag{6}$$

At each time step, we need to determine the magnitude of the electric field, denoted by $E_0(k)$. We assume that by applying a specific AC field with a fixed frequency, the rotating rate of each nanowire is constant. Therefore, we can compute the heading angles of the ith nanowire $\theta_i(k) = \theta_i(0)+\epsilon_i k\phi$, which includes a constant parameter ϕ and an independent variable ϵ_i that scales the nanowire's rotating speed. Thereby, the discrete-time system dynamics can be expressed in a simplified form:

$$\begin{bmatrix}x_i(k+1)\\ y_i(k+1)\end{bmatrix} = \begin{bmatrix}x_i(k)\\ y_i(k)\end{bmatrix} + \zeta_{ip}\begin{bmatrix}\cos(\theta_i(0)+\epsilon_i k\phi)\\ \sin(\theta_i(0)+\epsilon_i k\phi)\end{bmatrix}E_0(k)dt. \tag{7}$$

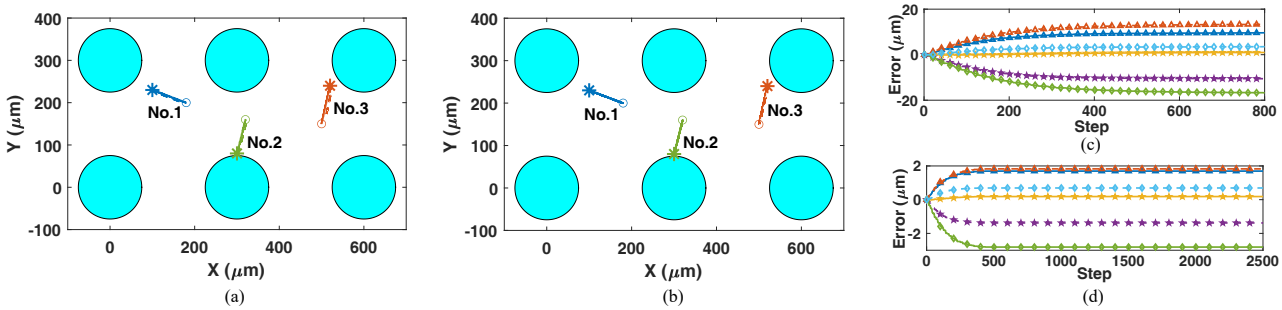

Fig. 4. Manipulation results for three nanowires using the two-stage control strategy. (a) Trajectory plot with $k = 800$. (b) Trajectory plot with $k = 2500$. The "*" and "o" markers indicate the nanowires' initial and target positions, respectively. "- -" is the actual trajectory, and "-" is the desired trajectory from the first stage. (c) Position errors plot with $k = 800$. (d) Position errors plot with $k = 2500$. "-△-" is the position error for nanowire No. 1. "-⋆-" is the position error for nanowire No. 2. "-◇-" is the position error for nanowire No. 3. "-" is the error in the x direction, and "- -" is the error in the y direction.

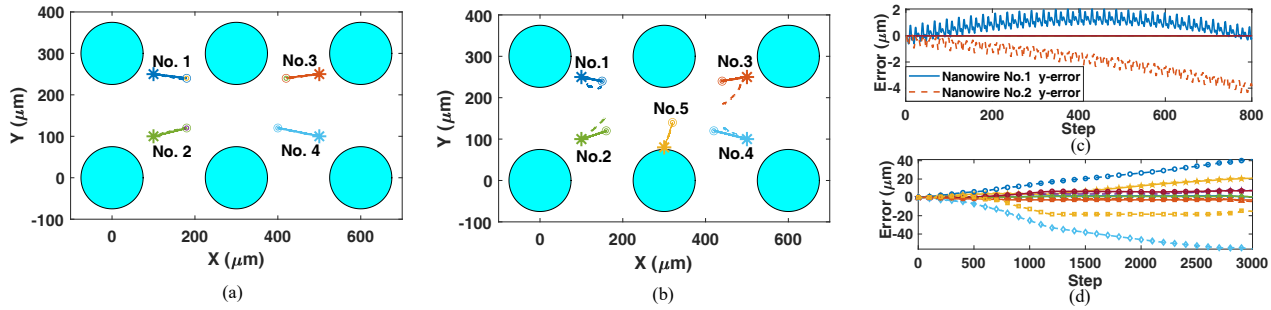

Fig. 5. Manipulation results for four and five nanowires using the two-stage control strategy. (a) Trajectory plot for the four nanowires. (b) Trajectory plot for the five nanowires. The markers "*" and "o" indicate initial and target positions, respectively. The dashed line ("- -") represents the actual trajectory, while the solid line ("-") represents the desired trajectory from the first stage. (c) Position error plot for the four nanowires. The errors along the x direction for all nanowires are close to zero. The errors in the y direction for nanowires 1 and 2 reach up to 4 μm during motion. (d) Position error plot for the five nanowires. The symbols "-△-", "-⋆-", "-◇-", "-o-", and "-□-" represent position errors for nanowires 1, 2, 3, 4, and 5, respectively. The solid line ("-") represents the error in the x direction, and the dashed line ("- -") represents the error in the y direction.

Similar as [20], we show the first stage of the system is uniformly k-step controllable by defining the controllability matrix $\mathcal{C}_k$. For the time step from 1 to k, the ith nanowire's position is updated as follows:

$$\begin{aligned}
\begin{bmatrix} x_i(1) \\ y_i(1) \end{bmatrix} &= \begin{bmatrix} x_i(0) \\ y_i(0) \end{bmatrix} + \zeta_{ip} \begin{bmatrix} \cos(\theta_i(0)) \\ \sin(\theta_i(0)) \end{bmatrix} E_0(0)dt, \\
\begin{bmatrix} x_i(2) \\ y_i(2) \end{bmatrix} &= \begin{bmatrix} x_i(1) \\ y_i(1) \end{bmatrix} + \zeta_{ip} \begin{bmatrix} \cos(\theta_i(0) + \epsilon_i\phi) \\ \sin(\theta_i(0) + \epsilon_i\phi) \end{bmatrix} E_0(1)dt, \\
&\vdots \\
\begin{bmatrix} x_i(k+1) \\ y_i(k+1) \end{bmatrix} &= \begin{bmatrix} x_i(k) \\ y_i(k) \end{bmatrix} + \zeta_{ip} \begin{bmatrix} \cos(\theta_i(0) + \epsilon_i k\phi) \\ \sin(\theta_i(0) + \epsilon_i k\phi) \end{bmatrix} E_0(k)dt.
\end{aligned} \tag{8}$$

From above, define the matrix $\hat{B}_i(k) = \zeta_{ip}[\cos(\theta_i(0) + \epsilon_i k\phi) \ \sin(\theta_i(0) + \epsilon_i k\phi)]^\intercal$ for each nanowire, and put them together for n nanowires at kth step, it has $\hat{\boldsymbol{B}}(k) = [\hat{B}_1(k)^\intercal, \hat{B}_2(k)^\intercal, \cdots, \hat{B}_n(k)^\intercal]^\intercal$. The controllability matrix $\mathcal{C}_k$ is defined by $\hat{\boldsymbol{B}}(k)$ shown as: $\mathcal{C}_k = [\hat{\boldsymbol{B}}(0), \hat{\boldsymbol{B}}(1), \ldots, \hat{\boldsymbol{B}}(k-1)]$. The control problem then becomes, for any starting state $\boldsymbol{p}_0$ and desired final state $\boldsymbol{p}_k$, solve for the control sequence $[E_0(0), E_0(1), \ldots, E_0(k-1)]$ subject to the constraint $\mathcal{C}_k[E_0(0), E_0(1), \ldots, E_0(k-1)] = (\boldsymbol{p}_k - \boldsymbol{p}_0)$. To make sure the $\mathcal{C}_k$ is not ill-conditioned, which would lead to very large control commands, we desire to pick a k at least $k \geqslant 4n$, where n is the number of the nanowires to be controlled. As a result, the matrix $\mathcal{C}_k$ is full rank, and because $k > 2n$, the system is underdetermined, with an infinite number of solutions. By using the Moore-Penrose pseudoinverse to solve the problem, it results in better numerical accuracy than the solution with minimal control effort [21].

2) Second Stage: After obtaining the electric field strength required to manipulate multiple nanowires to their targets in the first stage, a desired trajectory, $\boldsymbol{p}_f$, is generated by substituting the input to the system dynamics. In the second stage, we solve for the voltages necessary to follow the generated trajectory using the original system dynamics while satisfying the electric field constraints. To account for both the magnitude and direction of the electric fields and voltage bounds, we define the following optimal control problem to solve for the demand voltages:

$$\begin{aligned}
\min \quad & \sum_{j=1}^{k-1} \|\boldsymbol{p}(j) - \boldsymbol{p}_f(j)\|_2 \\
\text{subject to} \quad & \boldsymbol{p}(j+1) = \boldsymbol{p}(j) + \boldsymbol{Z}\boldsymbol{B}(\boldsymbol{p}(j))\boldsymbol{u}(j)dt, \\
& \quad j = 0, 1, \ldots, k-1 \\
& \|\boldsymbol{u}\|_\infty < u_{\text{bound}} \\
& \angle(\boldsymbol{B}(\boldsymbol{p}(i))\boldsymbol{u}) = \theta_i, \quad i = 1, 2, \ldots, n
\end{aligned} \tag{9}$$

3) Simulation Results: The maximum number of nanowires that can be independently manipulated by an $N \times N$ electrode array is limited to $N^2/2$ [22]. To overcome this limitation, the ensemble control strategy is crucial. In the simulation, we

used a 2×3 electrode array with a center-to-center distance of 300 μm as the actuators. The maximum number of nanowires that can be controlled for this setup is 3 [22]. To achieve precise and agile motion of the nanowires, it is suggested to put two nanowires in two different cells separately [23]. The two-stage open-loop ensemble control strategy expands the control limit to larger numbers. In the first stage, the number of nanowires that can be controlled is not limited due to the subsystem ensemble controllability. However, the original system dynamics and the constraints of the microfluidic system's physical properties limit the number of nanowires that the system can manipulate in the second stage. We explored the maximum limitation through simulation results. Fig. 4 shows the manipulation of three nanowires to their independent targets and the position errors between the actual and desired trajectories with input voltage bounded to 500 V. The maximum final position error is 16.7 μm in Fig. 4(c), and 2.81 μm in Fig. 4(d), where the control step k is 800 and 2500, respectively. The control step k significantly affects the control result. Insufficiently large k results in extremely large electric magnitude commands in the first stage, which cannot be generated by the limited control input from the second stage, leading to a final position error outside the target region.

Simulation results for controlling four and five nanowires are shown in Fig. 5. The control step for four nanowires is 800, and the maximum position error is 4.27 μm. For five nanowires, a larger control step of 3000 was used, but the manipulation was unsuccessful. Although the proposed two-stage open-loop method can break the control limits for six electrodes, it has several disadvantages, such as assuming known zeta potentials, requiring the determination of a suitable control step, and the possibility of instability due to the open-loop control.

C. Model Predictive Ensemble Control

In this section, we propose a closed-loop model predictive ensemble control method for manipulating multiple nanowires, using the same system dynamics as in Eq. (7). The model predictive ensemble control is formulated as:

$$\begin{aligned} \min \quad & \sum_{i=1}^{N_h-1} \|\boldsymbol{p}(i) - \boldsymbol{p}_k\|_Q \\ \text{subject to} \quad & \boldsymbol{p}(j+1) = \boldsymbol{p}(j) + \boldsymbol{Z}\boldsymbol{B}(\boldsymbol{p}(j))\boldsymbol{u}(j)dt \\ & \quad j = 0, 1, \ldots, k-1 \\ & \|\boldsymbol{u}\|_\infty < u_{\text{bound}} \\ & \angle(\boldsymbol{B}(\boldsymbol{p}(i))\boldsymbol{u}) = \theta_i, \quad i = 1, 2, \ldots, n \end{aligned} \tag{10}$$

The optimal control problem is solved for control inputs at each step. Unlike the open-loop ensemble control approach, this method does not require a desired trajectory to be generated for the control law to track. Instead, an optimal control problem with horizon length N_h is formulated to find the best solution for controlling the nanowires to different targets. To ensure ensemble controllability, we impose a constraint that the electric field direction at each nanowire's position must be aligned with the nanowire's orientation. This condition theoretically allows the control of up to N^2 nanowires using N^2 electrodes, as there is only one direction constraint for controlling each individual nanowire. The motion gain matrix $\boldsymbol{B}$ can have at most N^2 rows to avoid an overdetermined system that has no solution for the inputs. This breaks the limit of $N^2/2$ discussed previously. Assumptions for the two-stage open-loop ensemble control law are used, including known zeta potentials and fixed rotational rates. A 2×3 electrode array with an input voltage bound of 200 V is used in the simulations. Results in Figs. 6–8 show successful control of the nanowires to their target areas independently and simultaneously, breaking the maximum number of controlled nanowires. The controller takes 236, 1052, and 13700 steps to manipulate four, five, and six nanowires, respectively. However, it takes more steps to manipulate a larger number of nanowires independently. The electric field plots at different time steps show the generated electric field directions are aligned with the nanowires' orientations, as assumed in the model predictive ensemble control.

IV. Conclusion

In this work, a new microfluidic device setup is developed for ensemble control of nanowires. A rotational model for nanowires in fluid is derived and validated experimentally. The ensemble controllability is proved by generating a higher power of the distribution parameter using Lie brackets. Two control methods, the two-stage open loop ensemble control and the model predictive ensemble control, are proposed and demonstrated to break the limit on the maximum number of nanowires that can be simultaneously and independently controlled. The model predictive ensemble control method is able to manipulate up to six nanowires simultaneously to their independent targets. Future work involves fabricating the microfluidic device, developing an estimation method for unknown parameters in the control process, and conducting experiments to further validate the proposed control strategies.

References

[1] G. Adam, S. Chowdhury, M. Guix, B. V. Johnson, C. Bi, and D. Cappelleri, "Towards functional mobile microrobotic systems," *Robotics*, vol. 8, no. 3, p. 69, 2019.

[2] C. Pawashe, E. Diller, S. Floyd, and M. Sitti, "Assembly and disassembly of magnetic mobile micro-robots towards deterministic 2-d reconfigurable micro-systems," in *Proc. IEEE Int. Conf. Robot. Autom.*, Shanghai, China, 2011, pp. 261–266.

[3] Y. Kantaros, B. V. Johnson, S. Chowdhury, D. J. Cappelleri, and M. M. Zavlanos, "Control of magnetic microrobot teams for temporal micromanipulation tasks," *IEEE Trans. Robotics*, vol. 34, no. 6, pp. 1472–1489, 2018.

[4] E. Diller, S. Floyd, C. Pawashe, and M. Sitti, "Control of multiple heterogeneous magnetic microrobots in two dimensions on nonspecialized surfaces," *IEEE Trans. Robotics*, vol. 28, no. 1, pp. 172–182, 2011.

[5] D. DeVon and T. Bretl, "Control of many robots moving in the same direction with different speeds: a decoupling approach," in *Proc. Amer. Control Conf.*, St. Louis, MO, 2009, pp. 1794–1799.

[6] J.-S. Li and J. Qi, "Ensemble control of time-invariant linear systems with linear parameter variation," *IEEE Transactions on Automatic Control*, vol. 61, no. 10, pp. 2808–2820, 2015.

[7] A. Becker and T. Bretl, "Approximate steering of a unicycle under bounded model perturbation using ensemble control," vol. 28, no. 3, pp. 580–591, 2012.

[8] J.-S. Li and N. Khaneja, "Ensemble control of bloch equations," *IEEE Trans. Automat. Contr.*, vol. 54, no. 3, pp. 528–536, 2009.

[9] K. Yu, J. Yi, and J. W. Shan, "Automated characterization and assembly of individual nanowires for device fabrication," *Lab Chip*, vol. 18, no. 10, pp. 1494–1503, 2018.

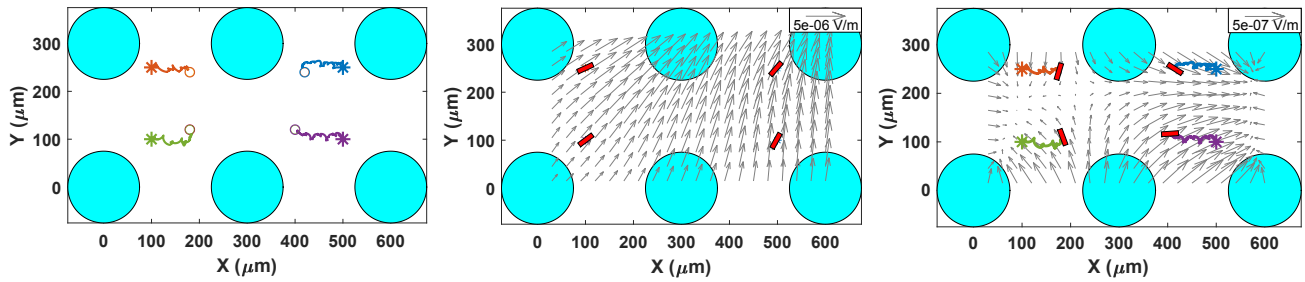

(a) (b) (c)

Fig. 6. (a) Manipulation results for four nanowires using the MPC ensemble control strategy. The "*" and "o" markers indicate the nanowire's initial and target positions, respectively. (b) The electric field at the 4th step of the control process. (c) The electric field at the 230th step of the control process.

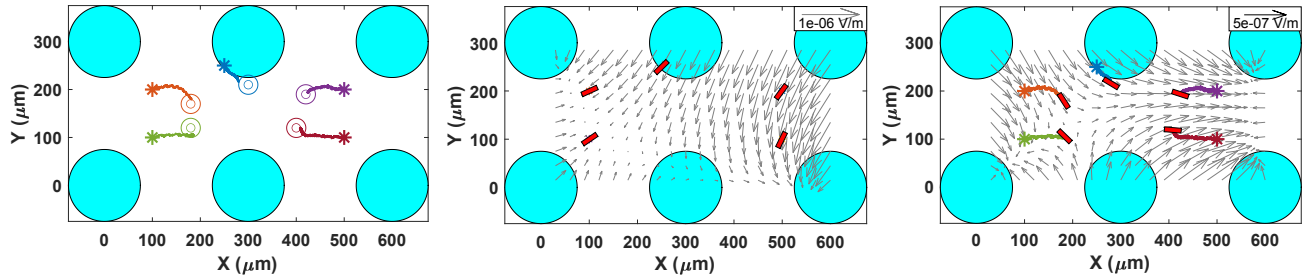

(a) (b) (c)

Fig. 7. (a) Manipulation results for five nanowires using the MPC ensemble control strategy. The "*" and "o" markers indicate the nanowire's initial and target positions, respectively. (b) The electric field at the 4th step of the control process. (c) The electric field at the 1050th step of the control process.

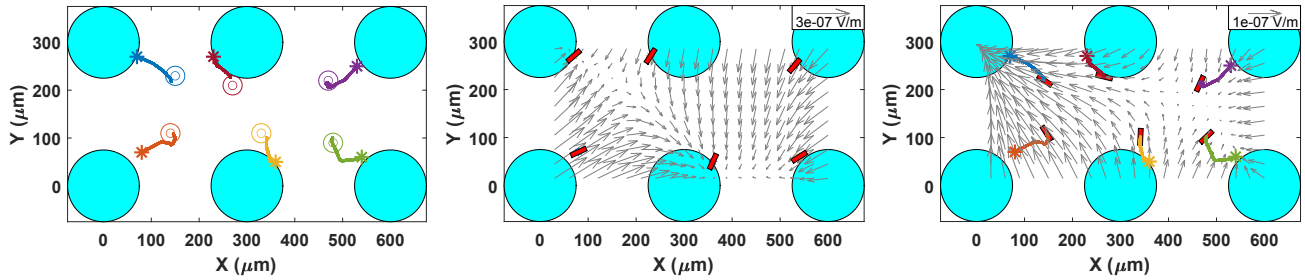

(a) (b) (c)

Fig. 8. (a) Manipulation results for six nanowires using the MPC ensemble control strategy. The "*" and "o" markers indicate the nanowire's initial and target positions, respectively. (b) The electric field at the 4th step of the control process. (c) The electric field at the 13700th step of the control process.

[10] T. B. Jones, *Electromechanics of Particles*. Cambridge, UK: Cambridge University Press, 2005.

[11] K. Yu, J. Yi, and J. Shan, "Motion control, planning and manipulation of nanowires under electric-fields in fluid suspension," *IEEE Trans. Automat. Sci. Eng.*, vol. 12, no. 1, pp. 37–49, 2015.

[12] K. Yu, J. Yi, and J. W. Shan, "Real-time motion planning of multiple nanowires in fluid suspension under electric-field actuation," *Int. J. Intell. Robot. Appl.*, vol. 2, no. 4, pp. 383–399, 2018.

[13] K. Yu, "Electrophoresis-based manipulation of micro-and nanoparticles in fluid suspensions," in *Field-Driven Micro and Nanorobots for Biology and Medicine*, Y. Sun, X. Wang, and J. Yu, Eds. Cham, Switzerland: Springer, 2022, pp. 133–164.

[14] D. Fan, F. Q. Zhu, R. C. Cammarata, and C.-L. Chien, "Controllable high-speed rotation of nanowires," *Physical Review Letters*, vol. 94, no. 24, p. 247208, 2005.

[15] D. Saintillan, E. Darve, and E. S. Shaqfeh, "Hydrodynamic interactions in the induced-charge electrophoresis of colloidal rod dispersions," *J. Fluid Mech.*, vol. 563, pp. 223–259, 2006.

[16] J. Wu, X. Li, and K. Yu, "Electrophoresis-Based Adaptive Manipulation of Nanowires in Fluid Suspension," *IEEE/ASME Trans. Mechatronics*, vol. 25, no. 2, pp. 638–649, 2020.

[17] J. Wu and K. Yu, "Adaptive tube model predictive control for manipulating multiple nanowires with coupled actuation in fluid suspension," in *Proc. IFAC World Congress*, Berlin, Germany, 2020, pp. 8734–8739.

[18] J. Wu and K. Yu, "Adaptive tube model predictive control of micro- and nanoparticles in fluid suspensions using global external fields," in *Proc. IEEE/ASME Int. Conf. Adv. Intelli. Mechatronics*, Delft, Netherlands, 2021, pp. 526–531.

[19] X. Li, J. Wu, J. Song, and K. Yu, "Informed Sampling-Based Motion Planning for Manipulating Multiple Micro Agents Using Global External Electric Fields," *IEEE Trans. Automat. Sci. Eng.*, vol. 19, no. 3, pp. 1422–1433, 2022.

[20] A. Becker, C. Onyuksel, T. Bretl, and J. McLurkin, "Controlling many differential-drive robots with uniform control inputs," *Int. J. Robot. Res.*, vol. 33, no. 13, pp. 1626–1644, 2014.

[21] R. Penrose, "A generalized inverse for matrices," *Mathematical Proceedings of the Cambridge Philosophical Society*, vol. 51, no. 3, pp. 406–413, 1955.

[22] K. Yu, J. Yi, and J. Shan, "Simultaneous multiple-nanowire motion control, planning, and manipulation under electric fields in fluid suspension," *IEEE Trans. Automat. Sci. Eng.*, vol. 15, no. 1, pp. 80–91, 2018.

[23] J. Wu and K. Yu, "Adaptive Tube Model Predictive Control for Manipulating Micro- and Nanoparticles in Fluid Suspensions Under Global External Fields," *IEEE Trans. Automat. Sci. Eng.*, 2022, early access. doi: 10.1109/TASE.2022.3187956.